

\mathcal{CP} ODD ANOMALOUS INTERACTIONS OF HIGGS BOSON IN ITS PRODUCTION AT PHOTON COLLIDERS

I.F. Ginzburg^{1,2*}, I.P. Ivanov^{1,2,3†}

¹ Institute of Mathematics, Novosibirsk, Russia

² Novosibirsk State University Novosibirsk, Russia

³ IKP, Forschungszentrum Jülich, Germany

Abstract

We discuss the potentialities of the study of \mathcal{CP} odd interactions of the Higgs boson with photons via its production at $\gamma\gamma$ and $e\gamma$ colliders. Our treatment of $H\gamma\gamma$ and $HZ\gamma$ anomalous interactions includes a set of parameters, whose impact on physical observables has not been considered before. We focus on two reactions — $\gamma\gamma \rightarrow H$ and $e\gamma \rightarrow eH$ — and introduce the polarization and/or azimuthal asymmetries that are particularly sensitive to specific features of anomalies. We discuss the ways of disentangling effects of physically different parameters of anomalies and estimate what magnitude of \mathcal{CP} violating phenomena can be seen in these experiments.

1 Introduction

In paper [1] we studied potentialities to discover \mathcal{CP} even anomalous interactions of the Higgs boson via its production at $\gamma\gamma$ and γe colliders. Below we bring under analysis effects of \mathcal{CP} -parity violating anomalies. They result in the polarization and azimuthal asymmetries in the Higgs boson production. With new opportunities for variation of photon polarization at Photon Colliders [2], the Higgs boson production at $\gamma\gamma$ and γe colliders has an exceptional potential in the extraction of these anomalies. To some extent, some similar issues have been considered in Refs. [3]–[8]. However, in the analysis there the polarization potential was not used in its complete form and some natural degrees of freedom in the parameter space were not considered. Besides, the authors cited consider either $\gamma\gamma$ or γe collisions separately. In the present paper we have in mind that experiments in $\gamma\gamma$ and γe collider modes will supplement each other and provide complementary opportunities in investigating Higgs boson anomalous interactions.

In our analysis we assume the Higgs boson to have been discovered before the photon collider starts operating, so that its basic properties will be known by that time. Our substantial idea is the necessity of step-by-step strategy in studying anomalous effects.

*E-mail: ginzburg@math.nsc.ru

†E-mail: i.ivanov@fz-juelich.de

Namely, the first step is the study of $H\gamma\gamma$ anomalies in $\gamma\gamma$ collisions and the second step is using γe collisions for the study of $HZ\gamma$ anomalies assuming $H\gamma\gamma$ anomalies (both \mathcal{CP} even and \mathcal{CP} odd) to be studied at the first stage (with higher accuracy than it is possible at the second stage).

The $\gamma\gamma$ and γe colliders will be the specific modes of the future Linear Colliders (in addition to the e^+e^- mode) with the following typical parameters (*which can be obtained without a specific optimization for the photon mode*) [9, 10] (E and \mathcal{L}_{ee} are the electron energy and luminosity of the basic e^+e^- collider).

- *Characteristic photon energy $E_\gamma \approx 0.8E$.*
- *Annual luminosity $\mathcal{L}_{\gamma\gamma} \approx 0.2\mathcal{L}_{ee}$, typical $\mathcal{L}_{\gamma\gamma} \approx 100 \text{ fb}^{-1}$.*
- *Mean energy spread $\langle \Delta E_\gamma \rangle \approx 0.07E_\gamma$.*
- *Mean photon helicity $\langle \lambda_\gamma \rangle \approx 0.95$ with variable sign [9].*
- *Circular polarization of photons can be transformed into the linear one [2].*

The effective photon spectra for these colliders are given in Ref. [11]. With the above properties, considering photon beams at the Photon Collider as roughly monochromatic is good approximation for our purposes.

The value of effects which can be observed in experiment is given by the expected accuracy in the measuring of the cross sections under interest. For the $\gamma\gamma$ colliders the expected accuracy in the measuring of Higgs boson decay width will be 2% or better [12]. For $e\gamma \rightarrow eH$ process we estimate the achievable accuracy to be 5 \div 10%.

Throughout the paper we denote by λ and $\zeta/2$ the average helicities of photons and electrons and by ℓ the average degree of the photon linear polarization. We use some \mathcal{SM} notation: $s_W = \sin \theta_W$, $c_W = \cos \theta_W$, $v_e = 1 - 4 \sin^2 \theta_W$ and $v = 246 \text{ GeV}$ (Higgs field v.e.v.). In the numerical calculations we assume the Higgs boson to lie in the most expected mass interval 100–250 GeV. Some further notations are borrowed from ref. [1].

2 Sources of \mathcal{CP} violation. The Effective Lagrangian

One can imagine two possible sources of \mathcal{CP} violation in the interactions of the Higgs boson. First, the observed Higgs boson can mix with some pseudoscalar field, as it can happen in the two-doublet Higgs model or in \mathcal{MSM} , see for details, e.g. [3, 13]. In this case \mathcal{CP} violating effects could be strong. A certain variant of this opportunity is considered in Sec. 5.

The second possibility, which is our major concern here, is that the Higgs boson itself is \mathcal{CP} even fundamentally but underlying interactions can break the \mathcal{CP} parity conservation law. In this case we expect small \mathcal{CP} violating effects. One can describe them by the Effective Lagrangian which is expanded in some large energy scale Λ .

Effective Lagrangian and its parameters. The items of dimension 6 in the Effective Lagrangian are well known (see e.g. [14, 15]). Just as in ref. [1], these anomalies can be summarized for our problem in the expression

$$\Delta\mathcal{L} = (2Hv + H^2) \left(\theta_\gamma \frac{F_{\mu\nu}F^{\mu\nu}}{2\Lambda_\gamma^2} + \theta_Z \frac{Z_{\mu\nu}F^{\mu\nu}}{\Lambda_Z^2} + i\theta_{P\gamma} \frac{F_{\mu\nu}\tilde{F}^{\mu\nu}}{2\Lambda_{P\gamma}^2} + i\theta_{PZ} \frac{Z_{\mu\nu}\tilde{F}^{\mu\nu}}{\Lambda_{PZ}^2} \right), \quad (| \theta_i | = 1). \quad (1)$$

Here $F^{\mu\nu}$ and $Z^{\mu\nu}$ are the standard field strengths for the electromagnetic and Z field and $\tilde{F}^{\mu\nu} = \varepsilon^{\mu\nu\alpha\beta} F_{\alpha\beta}/2$.

In the case of \mathcal{CP} conservation, all coefficients of Lagrangian are real, in particular, $\theta_i = \pm 1$. This Ansatz is often used even in the \mathcal{CP} violation case. However, in this case this limitation breaks down, so that parameters θ_i can be complex

$$\theta_i = e^{i\xi_i} \quad (i = \gamma, Z, P\gamma, PZ). \quad (2)$$

These new degrees of freedom have not been considered in the previous papers. The extraction of these phases should be an additional subject of the data analysis.

The scales Λ_i are just parameters in Eq. (1) and their relation to the energy scale of the underlying New Physics phenomena Λ_{NP} depends on the details of underlying interactions. For instance, one can have $\Lambda_{NP} \approx e\Lambda$ or $\Lambda_{NP} \sim (e/2\pi)\Lambda$ or even $\Lambda_{NP} \sim \Lambda/e$, where $e \approx 0.3$ is the electron electric charge. The first case can correspond to existence of an additional Z' boson interacting with Higgs field as BHZ' before symmetry breaking. The second relation can describe the case of loops with heavy particles within the effective vertex. The third case corresponds to Higgs boson-photon effective interaction via the point-like Dirac monopole loops.

Our particular parameterization can be readily linked to that used in other papers (e.g.[6, 14, 15]). For example, correspondence of our parameters Λ_i to dimensionless constants used in ref. [6] reads $d_{Z\gamma} = (4\theta_Z/(c_W s_W))(v^2/\Lambda_Z^2)$, $\bar{d}_{Z\gamma} = (2\theta_{PZ})(c_W s_W)(v^2/\Lambda_{PZ}^2)$.

Since we deal with 3-field interaction, one can write in this very form the entire Effective Lagrangian, which describes $H\gamma\gamma$ and $HZ\gamma$ interactions and includes both \mathcal{SM} and anomalous terms:

$$\mathcal{L}_{eff} = \mathcal{L}_{eff}(\gamma\gamma H) + \mathcal{L}_{eff}(\gamma Z H) \quad (3)$$

$$\mathcal{L}_{eff}(\gamma\gamma H) = \frac{1}{2v} \left[G_\gamma H F^{\mu\nu} F_{\mu\nu} + i\tilde{G}_\gamma H F^{\mu\nu} \tilde{F}_{\mu\nu} \right]$$

$$\mathcal{L}_{eff}(\gamma Z H) = \frac{1}{v} \left[G_Z H F^{\mu\nu} Z_{\mu\nu} + i\tilde{G}_Z H F^{\mu\nu} \tilde{Z}_{\mu\nu} \right]. \quad (4)$$

with effective coupling constants:

$$G_i = G_i^{SM} + 2\theta_i \frac{v^2}{\Lambda_i^2}, \quad \tilde{G}_i = 2\theta_{Pi} \frac{v^2}{\Lambda_{Pi}^2}. \quad (5)$$

Their \mathcal{SM} values G_i^{SM} are well known, see e.g. [1] for normalization. (With the proposed experimental accuracy, when doing the final numerical calculation, one should, of course, use $\gamma\gamma H$ coupling with radiative corrections [16]). The imaginary parts of these coefficients become large even without \mathcal{CP} violation, for example, in the Two Doublet Higgs Model (II) or in \mathcal{MSSM} at large $\tan\beta$ due to enhanced contribution of b -quark loops¹.

¹ Certainly, only phase differences are measurable for these entire effective couplings. Expecting relatively small magnitude of anomaly, one can conclude that the phases of entire quantities G_γ , G_Z are close to their \mathcal{SM} values ξ_γ^{SM} and ξ_Z^{SM} and the effect of anomaly itself is reduced by factor $\cos(\xi_\gamma - \xi_\gamma^{SM})$. The study of dependence on an additional variable like the transferred momentum in $e\gamma \rightarrow eH$ process can provide here new information via the details of interference effects.

Effect of higher dimension operators. The Effective Lagrangians (3),(4) include only dimension 6 anomalous terms, i.e. they have $(v/\Lambda_i)^2$ accuracy; terms of dimension 8, which are $\sim (v/\Lambda)^4$, are neglected here. Thus, in this approximation we cannot, strictly speaking, study contributions of $|\tilde{G}_\gamma|^2$ and $|\tilde{G}_Z|^2$ to the cross sections, because their effect would be of the same order as interference of neglected $dim = 8$ terms with the \mathcal{SM} contribution.

Fortunately, for the $H\gamma\gamma$ Effective Lagrangian (as well as for other 3-field vertices) this limitation can be avoided. Indeed, if we fix the external fields, then the structure of *any possible higher dimension operator* can be reduced to those in (3) by integrating by parts in the effective action and exploiting the free equations of motion. In other words, all operators of higher dimension with the same set of physical fields will have form (3) and their addition to (3) can be considered as a simple (and arguably small) renormalization of parameters Λ in eq. (3). In this sense we consider Eq.(3) as the precise Effective Lagrangian of the $\gamma\gamma H$ interaction. Note however that the strict relation between $2Hv$ and H^2 items in (1) is broken now.

The $HZ\gamma$ coupling is determined from reaction $e\gamma \rightarrow eH$ where additional physical fields are involved. Therefore, the above conclusion cannot be used here. Indeed, for example, dimension 7 operators like $\bar{\ell}\sigma^{\mu\nu}\ell F_{\mu\nu}\phi^2$, etc. should be added in the analysis at higher accuracy. Note that this difficulty is inessential for our problem since the magnitude of such corrections as well as of the $|\tilde{G}_i|^2$ contribution lies far below the attainable accuracy in determination of $HZ\gamma$ coupling.

About figures and notation there. Currently, due to the large number of new model parameters, a thorough investigation of regions of the parameter space, achievable in future experiments, makes little sense. Instead of that we present in our figures examples for some values of parameters, which illustrate that the study of these effects at the Photon Colliders is indeed possible and profitable.

There are no doubts that relatively large anomalies will be discovered easily. Therefore, we will concentrate our efforts on the most natural case when the anomalous effects are relatively small as compared with basic \mathcal{SM} effects (i.e. the scale of New Physics is large). In this case the effects of anomalies will be seen mainly in the interference with the \mathcal{SM} effects. In this approximation contributions of different anomalies in the observed cross sections are additive with good accuracy. This is why we treat each anomaly separately, assuming all other anomalies absent (the corresponding $\Lambda_i = \infty$).

3 Process $\gamma\gamma \rightarrow H$

Let us denote by $\langle\sigma^{SM}\rangle_{np}$ the \mathcal{SM} Higgs boson production cross section in unpolarized photon collisions averaged over a certain small effective mass interval (see e.g. [1]) and by ψ the angle between directions of linear polarization of the two photons. Then the cross

section of the Higgs boson production can be written in the form:

$$\langle\sigma\rangle(\lambda_i, \ell_i, \psi) = \langle\sigma^{SM}\rangle_{np} T(\lambda_i, \ell_i, \psi);$$

$$T(\lambda_i, \ell_i, \psi) = \frac{|G_\gamma|_{}^2}{|G_\gamma^{SM}|_{}^2} (1 + \lambda_1 \lambda_2 + \ell_1 \ell_2 \cos 2\psi) + \frac{|\tilde{G}_\gamma|_{}^2}{|G_\gamma^{SM}|_{}^2} (1 + \lambda_1 \lambda_2 - \ell_1 \ell_2 \cos 2\psi) \quad (6)$$

$$+ 2 \frac{Re(G_\gamma^* \tilde{G}_\gamma)}{|G_\gamma^{SM}|_{}^2} (\lambda_1 + \lambda_2) + 2 \frac{Im(G_\gamma^* \tilde{G}_\gamma)}{|G_\gamma^{SM}|_{}^2} \ell_1 \ell_2 \sin 2\psi.$$

In the \mathcal{SM} case we have only the first item in this sum. (Note that the $\gamma\gamma \rightarrow b\bar{b}$ background is practically independent on linear polarization of photons.)

An important feature here is interference terms. They give rise to the inequality of the two directions of rotation and to the modification of the ψ -dependence, which is entirely due to the \mathcal{CP} odd admixture to \mathcal{CP} even Lagrangian. Owing to these modifications, a number of experimentally measurable quantities appear that can help study \mathcal{CP} even and odd anomalies separately.

It is useful to introduce five different asymmetries:

$$T_{\pm} = \frac{\langle\sigma\rangle(\lambda_i, \ell_i = 0) \pm \langle\sigma\rangle(-\lambda_i, \ell_i = 0)}{2\langle\sigma^{SM}\rangle_{np}} \propto \begin{cases} (1 + \lambda_1 \lambda_2)(|\tilde{G}_\gamma|_{}^2 + |G_\gamma|_{}^2), \\ 2(\lambda_1 + \lambda_2)Re(\tilde{G}_\gamma^* G_\gamma); \end{cases}$$

$$T_{\parallel} = \frac{\langle\sigma\rangle(\lambda_i = 0, \ell_i, \psi = 0)}{\langle\sigma^{SM}\rangle_{np}} \propto [|G_\gamma|_{}^2(1 + \ell_1 \ell_2) + |\tilde{G}_\gamma|_{}^2(1 - \ell_1 \ell_2)],$$

$$T_{\perp} = \frac{\langle\sigma\rangle(\lambda_i = 0, \ell_i, \psi = \pi/2)}{\langle\sigma^{SM}\rangle_{np}} \propto [|G_\gamma|_{}^2(1 - \ell_1 \ell_2) + |\tilde{G}_\gamma|_{}^2(1 + \ell_1 \ell_2)],$$

$$T_{\psi} = \frac{\langle\sigma\rangle(\lambda_i = 0, \ell_i, \psi = 3\pi/4) - \langle\sigma\rangle(\lambda_i = 0, \ell_i, \psi = \pi/4)}{\langle\sigma^{SM}\rangle_{np}} \propto 2\ell_1 \ell_2 Im(\tilde{G}_\gamma^* G_\gamma), \quad (7)$$

whose \mathcal{SM} values are

$$T_+^{SM} = 1 + \lambda_1 \lambda_2, \quad T_-^{SM} = 0, \quad T_{\parallel}^{SM} = 1 + \ell_1 \ell_2, \quad T_{\perp}^{SM} = 1 - \ell_1 \ell_2, \quad T_{\psi}^{SM} = 0.$$

The quantities T_+ , T_{\parallel} and T_{\perp} are combinations of $|G_\gamma|_{}^2$ and $|\tilde{G}_\gamma|_{}^2$ with different weights. These asymmetries are sensitive to the \mathcal{CP} even anomaly and its phase ξ_γ via its interference with the \mathcal{SM} contribution. The best quantity for this study is of course T_+ , which is illustrated by Fig. 1. Certainly, curves for \mathcal{CP} even anomaly effects at $\xi_\gamma = 0$ are the same as obtained in Ref. [1]. These three quantities include also the \mathcal{CP} odd anomaly in the form $|\tilde{G}_\gamma|_{}^2$, which is $\sim 1/\Lambda_{P\gamma}^4$, i.e. small and independent of $\xi_{P\gamma}$ (the corresponding $\Lambda_{P\gamma}$ dependence was studied in ref. [5]). Even in the case of T_{\perp} , where the contribution of $|\tilde{G}_\gamma|_{}^2$ is enhanced, it is difficult to see the effect of \mathcal{CP} -odd anomalies at reasonably large $\Lambda_{P\gamma}$, Fig.3.

The remaining two quantities — T_- and T_{ψ} — are much more useful for study of \mathcal{CP} violating effects in $\gamma\gamma H$ interaction. Their study supplements each other. Both of them differ from zero only if the \mathcal{CP} parity is broken. They derive from the interference of the \mathcal{CP} odd and \mathcal{CP} even items in \mathcal{L}_{eff} . Fig. 2 shows the T_- dependence on the scale $\Lambda_{P\gamma}$ and phase $\xi_{P\gamma}$ for different values of the Higgs boson mass. At $M_H < 160$ GeV (WW threshold) the basic quantity G_γ^{SM} is practically real. Therefore, the quantity T_- has maximum at $\xi_{P\gamma} = 0$. Above this threshold the imaginary part of G_γ^{SM} becomes substantial, and the position of maximum is shifted to $\xi_{P\gamma} \neq 0$. Fig. 4 shows that the

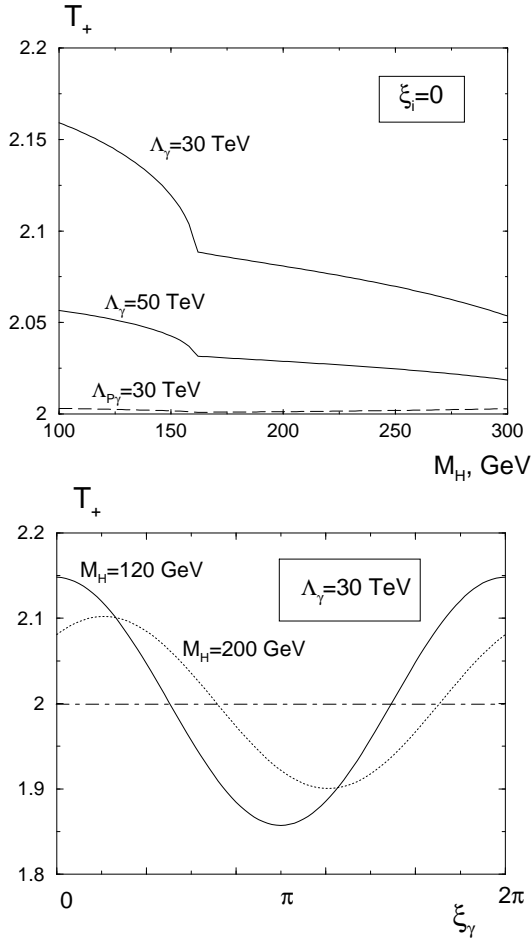


Figure 1: The quantity T_+ ; $\lambda_1\lambda_2 = 1$

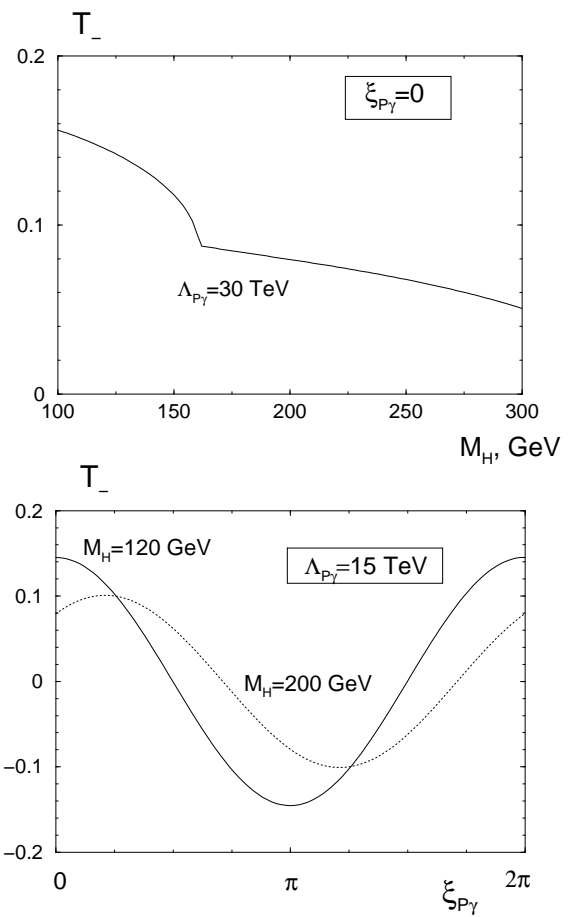


Figure 2: The quantity T_- ; $\lambda_1\lambda_2 = 1$

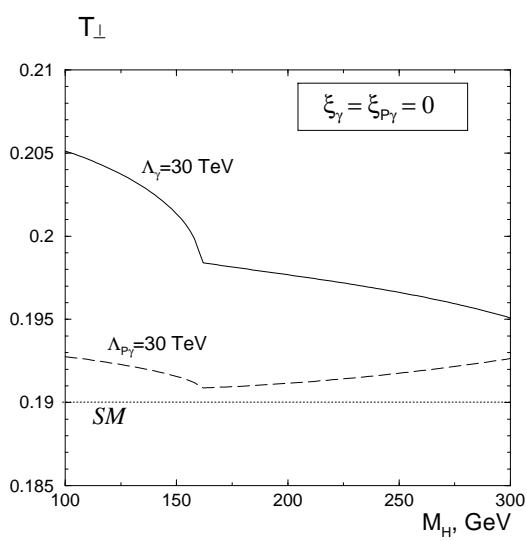


Figure 3: The quantity T_\perp ; $\ell_i = 0.9$

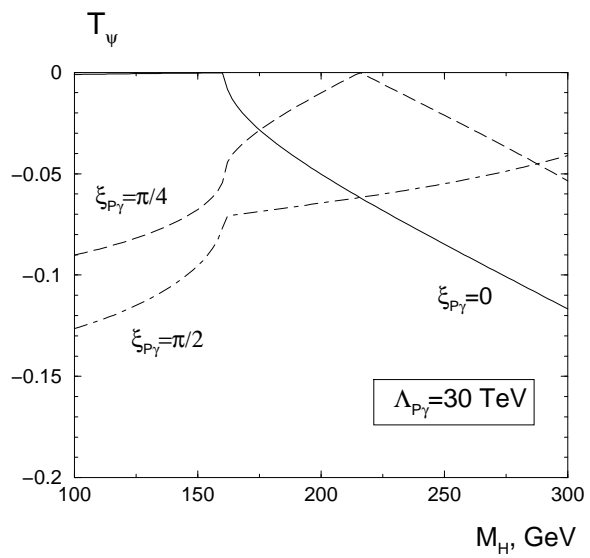


Figure 4: The quantity T_ψ ; $\ell_i = 0.9$

\mathcal{CP} odd anomaly effect is strong in this asymmetry as well, and exhibits a remarkable dependence of T_ψ on the value of phase $\xi_{P\gamma}$. With measurement of T_- and T_ψ one can extract from the data both $\Lambda_{P\gamma}$ and $\xi_{P\gamma}$ since T_- and T_ψ represent the real and imaginary part of the same quantity.

4 Process $e\gamma \rightarrow eH$

The process $e\gamma \rightarrow eH$ is considered here as a good tool for study of $HZ\gamma$ anomalous interactions provided $H\gamma\gamma$ anomalies are known from the experiments in the $\gamma\gamma$ mode. This process was studied within \mathcal{SM} in detail in refs. [1, 17]². It is described by diagrams of three types — those with photon exchange in t -channel, with Z exchange in t channel and box diagrams. This subdivision is approximately gauge invariant with accuracy $\sim m_e/M_Z$ [1]. The difference in the cross sections σ^L and σ^R for the left-hand and right-hand polarized electrons is obliged to interference between photon and Z exchange amplitudes.

The main contribution into the total cross section is given by diagrams with photon exchange in t -channel. Therefore, this total cross section is sensitive to the $H\gamma\gamma$ anomalies and weakly sensitive to the $HZ\gamma$ anomalies, which are our major concern here (the difference $\sigma^L - \sigma^R$ is small as compared with the unpolarized cross section). This picture is improved with the growth of transverse momentum of the scattered electron p_\perp . Indeed, with this growth photon exchange contribution is strongly reduced, while Z -boson exchange contribution changes only marginally at $p_\perp \lesssim M_Z$. At transverse momenta of the scattered electrons $p_\perp > 30$ GeV and for longitudinally polarized initial electrons the effect of Z -exchange should be seen well [1]. To feel the scale of observed effects, we present in Fig. 5 the \mathcal{SM} cross sections σ^L and σ^R integrated over the region $Q^2 > 1000$ GeV² and averaged over initial photon polarizations. We use this limitation in Q^2 everywhere below.

We denote the particle momenta as p for the incident electron, k for the photon, $p' = p - q$ for the scattered electron and $Q^2 = -q^2$. In our calculations far from the photon pole in t -channel we neglect the electron mass. We also denote: $u = 2kp' = M_H^2 + Q^2 - s$, $x = 2kq/s \equiv (M_H^2 + Q^2)/s$, $E_{tot} = \sqrt{s}$. The collision axis is labeled as z axis and x axis is chosen along the direction of the photon linear polarization vector $\vec{\ell}$. Finally, angle ϕ is the azimuthal angle of the scattered electron relative to so-defined x axis. The values $\zeta = -1$ or $\zeta = +1$ correspond to left-hand or right-hand polarized initial electrons. We use superscripts L and R to label quantities referring to these polarizations.

The qualitative features of the observable effect could be understood taking into account that the quantities below could be treated as the average helicity λ_V and degree of linear polarization ℓ_V of an exchanged virtual photon or Z boson:

$$\lambda_V = \frac{s^2 - u^2}{s^2 + u^2} \zeta = \frac{x - x^2/2}{1 - x + x^2/2} \zeta, \quad \ell_V = \frac{2s|u|}{s^2 + u^2} = \frac{1 - x}{1 - x + x^2/2}, \quad (8)$$

with vector of linear polarization $\vec{\ell}_V$ lying in the electron scattering plane [20]. Since usually $x \ll 1$, we have $\lambda_V \ll 1$ and $\ell_V \approx 1$. Therefore, joining the results of the previous

² The production of the pseudoscalar Higgs boson in such a reaction was studied e.g. in ref. [18], see also ref. [19] for the \mathcal{MSSM} case.

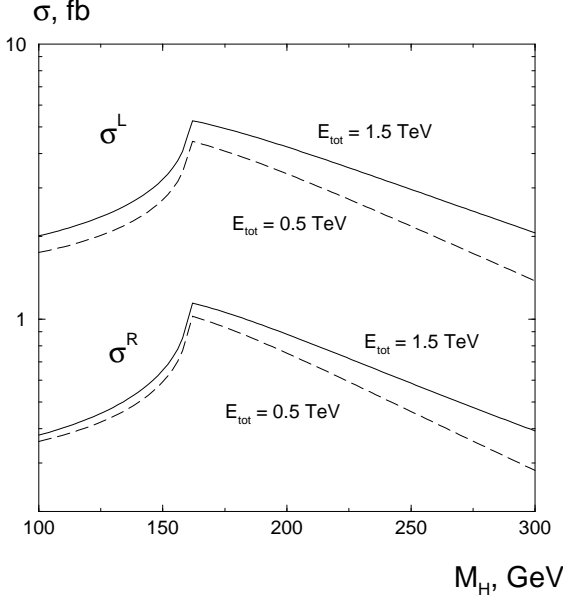


Figure 5: The SM cross section of $e\gamma \rightarrow eH$ process, $Q^2 > 1000$ GeV 2 .

section and those from ref.[1], one can conclude that the effect of \mathcal{CP} odd $HZ\gamma$ interaction can be seen in the dependence on angle ϕ in the experiments with left- and right-polarized electrons and in the study of dependence on the sign of the incident photon helicity. These dependences have not been studied earlier.

Helicity amplitudes of the process are calculated just as in Ref. [1]. With notations for the box contributions from that paper we have (in these equations helicities $\lambda, \zeta = \pm 1$)

$$\mathcal{M} = -\frac{4\pi\alpha}{M_W s_W} \sqrt{\frac{Q^2}{2}} \left\{ s \frac{1+\zeta\lambda}{2} + (s - M_H^2 - Q^2) \left[\frac{1-\zeta\lambda}{2} \cos 2\phi + \frac{\zeta-\lambda}{2} i \sin 2\phi \right] \right\} \times (\lambda K + \tilde{K}), \quad (K = V - \zeta A + B_+, \quad \tilde{K} = \tilde{V} - \zeta \tilde{A} + \zeta B_-). \quad (9)$$

Here V and A stand for vector and axial t -channel exchange contributions, B_{\pm} are the box contributions which are composed from items related to the W or Z circulating in box³:

$$\begin{aligned} V &= \frac{G_Z}{Q^2} + \frac{v_e G_Z}{4s_W c_W (Q^2 + M_Z^2)}, \quad A = -\frac{G_Z}{4s_W c_W (Q^2 + M_Z^2)}, \\ \tilde{V} &= \frac{\tilde{G}_Z}{Q^2} + \frac{v_e \tilde{G}_Z}{4s_W c_W (Q^2 + M_Z^2)}, \quad \tilde{A} = -\frac{\tilde{G}_Z}{4s_W c_W (Q^2 + M_Z^2)}; \\ B_{\pm} &= \frac{\alpha M_W^2}{4\pi s_W^2} \cdot \left[\frac{W(s, u) \pm W(u, s)}{2} + \frac{Z(s, u) \pm Z(u, s)}{2} \right]. \end{aligned} \quad (10)$$

The amplitude squared for an arbitrarily polarized photon beam can be written in terms of helicity amplitudes and the photon density matrix ρ written in helicity basis as

$$|\mathcal{M}|^2 = \mathcal{M}_a^* \rho_{ab} \mathcal{M}_b, \quad a, b = +, -, \quad \rho = \frac{1}{2} \begin{pmatrix} 1 + \lambda & -\ell \\ -\ell & 1 - \lambda \end{pmatrix}. \quad (11)$$

³ The box diagrams contribution (and their interference with other diagrams) is small in comparison with other contributions.

So that the cross section reads (here $\zeta = \pm 1$):

$$\begin{aligned} d\sigma = & \frac{\pi\alpha^2}{2M_W^2 s_W^2} \frac{d\phi}{2\pi} Q^2 dQ^2 \frac{s^2 + u^2}{2s^2} (U_0 + \lambda U_\lambda + \ell \cos 2\phi U_\perp - \ell \sin 2\phi U_\psi) ; \\ U_0 = & \left(|K|^2 + |\tilde{K}|^2 \right) + \lambda_V 2\text{Re} \left(K\tilde{K}^* \right), \quad U_\perp = \ell_V \left(|K|^2 - |\tilde{K}|^2 \right) \\ U_\lambda = & 2\text{Re} \left(K\tilde{K}^* \right) + \lambda_V \left(|K|^2 + |\tilde{K}|^2 \right), \quad U_\psi = 2\text{Im} \left(K\tilde{K}^* \right) . \end{aligned} \quad (12)$$

With notations (8) it becomes evident that this equation reproduces term by term the polarization dependencies of $\gamma\gamma \rightarrow H$ process (6), in particular, $T_+, T_{\parallel} \rightarrow U_0$, $T_{\perp} \rightarrow U_{\perp}$, $T_- \rightarrow U_\lambda$, $T_\psi \rightarrow U_\psi$. Therefore, the similar studies of $HZ\gamma$ interaction are possible here. However, there is a difference between effects of linear photon polarization in these two reactions. In the $\gamma\gamma$ collisions we can control linear polarizations and *choose* their relative orientation to study specific contribution. In the γe collision we cannot control relative orientation of linear polarizations, so that some Fourier-type analysis is necessary to see contributions under interest.

Different asymmetries. The quantities U_0 and U_{\perp} are weakly sensitive to the \tilde{G}_Z . The sensitivity of U_0 to the \mathcal{CP} even anomalous interaction was studied, in fact, in refs. [1, 6].

The quantities U_λ and U_ψ are most sensitive to the \mathcal{CP} odd anomalies. Thus, we consider asymmetries

$$\begin{aligned} V_\lambda^{L,R} &= \frac{\int d\sigma^{L,R}(\lambda) - \int d\sigma^{L,R}(-\lambda)}{|\lambda| \int d\sigma_{np}^{SM}} \propto \int U_\lambda^{L,R} , \\ V_\psi^{L,R} &= \frac{\int d\sigma^{L,R} \sin 2\phi}{|\ell| \int d\sigma_{np}^{SM}} \propto \int U_\psi^{L,R} , \end{aligned} \quad (13)$$

with integrations spanning over the region $Q^2 > Q_0^2 = 1000$ GeV 2 and the whole region of ϕ for the left-hand and right-hand polarized initial electrons. (The integrals in denominators are calculated for the nonpolarized initial particles.) It happens that the cross sections for the left-hand polarized electrons are much higher than those for the right-handed electrons (see Fig. 5). Therefore, we present graphs for the left-handed electrons only. The anomalous effect for the right-handed electrons is also small in its absolute value. We have not encountered any case where σ^R would be a useful source of additional information, despite the relative value of anomaly contribution can be higher here.

The quantity V_λ^L describing the helicity asymmetry is analogous to T_- in the $\gamma\gamma$ case with accuracy to contribution $\sim (|K|^2 + |\tilde{K}|^2)$ entering with small coefficient λ_V . This contribution results in non-zero V_λ even in \mathcal{SM} . Figs. 6 shows dependence of this quantity on Λ_{PZ} . For the purposes of comparison, the effect of a $\Lambda_{P\gamma} = 20$ TeV $H\gamma\gamma$ anomaly is also shown. We see that the values of this helicity asymmetry are large enough. Note that the signal/background ratio improves with the growth of energy since the \mathcal{SM} contribution into the discussed quantity decreases approximately $\propto \lambda_V \sim s^{-1}$ while the anomaly effect increases weakly, $\propto \ln(s/M_Z^2)$.

The same figure depicts also **the quantity V_ψ^L** at different values of Λ_{PZ} . Again we also draw a comparison with a $H\gamma\gamma$ \mathcal{CP} -odd anomaly. This quantity is intrinsically smaller than V_λ^L , so the \mathcal{CP} -odd $HZ\gamma$ anomaly can be seen only at $\Lambda_{PZ} \leq 10$ TeV.

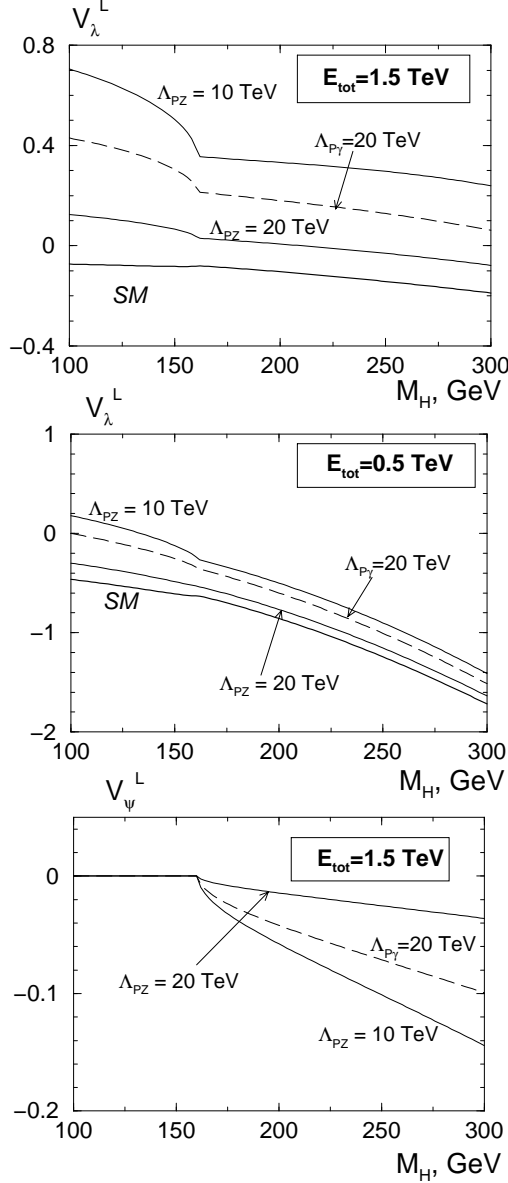


Figure 6: The asymmetries V_λ and V_ψ ; $Q^2 > 1000$ GeV 2 , $\xi_{P\gamma} = \xi_{PZ} = 0$

The dependence of V_λ and V_ψ on the phase of $HZ\gamma$ anomaly ξ_{PZ} is shown in Fig. 7. (The dependence of these quantities on the parameters of $H\gamma\gamma$ anomaly has the same form but the magnitude is somewhat larger.) These curves closely resemble dependences of T_- and T_ψ on $\xi_{P\gamma}$ in the $\gamma\gamma \rightarrow H$ case. We see the familiar phase dependence $\propto \cos(\xi_{PZ} - \bar{\xi}_\gamma)$ or $\sin(\xi_{PZ} - \bar{\xi}_\gamma)$ (here $\bar{\xi}_i$ are phases of G_γ and G_Z which are close to their SM values). The effect of switching on of the imaginary part of the SM contribution at $M_H \sim 160$ GeV is clearly seen in these curves. In the phenomenological analysis, it is very helpful that V_λ and V_ψ are intrinsically complementary: just as it was in $\gamma\gamma \rightarrow H$ case, V_λ is the real part and V_ψ is the imaginary part of the same quantity. Therefore, at any value of M_H and ξ_{PZ} either V_λ or V_ψ will deviate strongly from the SM value.

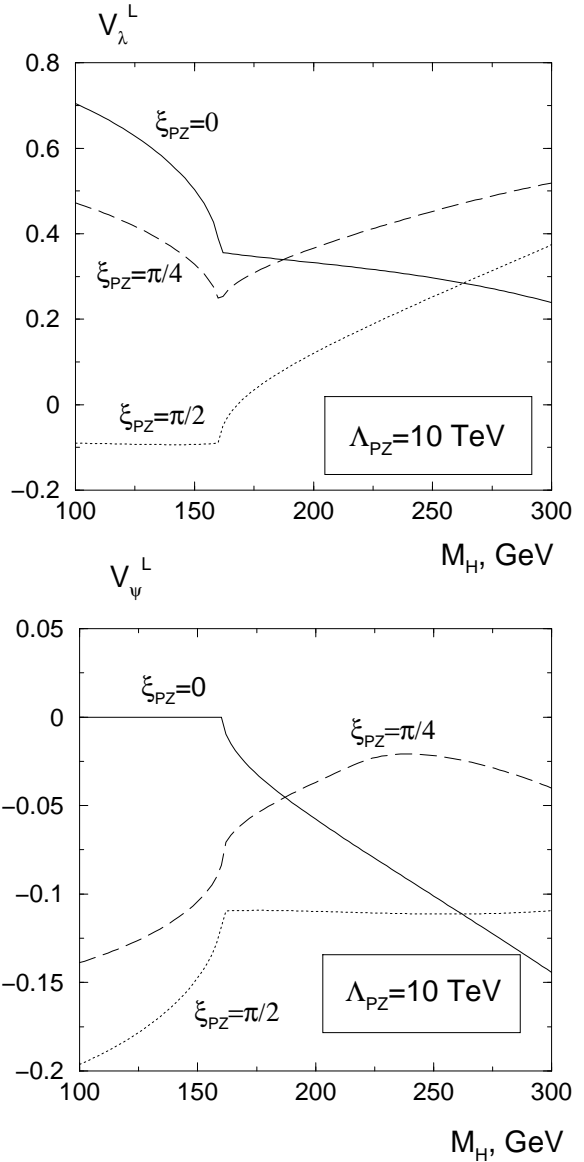


Figure 7: The asymmetries V_λ^L and V_ψ at different ξ_{Pi} , $Q^2 > 1000$ GeV 2

5 Scalar-pseudoscalar mixing within two doublet Higgs model

A specific case of \mathcal{CP} violation takes place in the scalar–axial mixing within the two doublet Higgs model (2HDM). This model is described with the aid of mixing angle β (defined via the ratio of v.e.v.’s for two basic scalar fields, $\tan \beta = \langle \phi_1 \rangle / \langle \phi_2 \rangle$) and three Euler mixing angles $\alpha_1, \alpha_2, \alpha_3$ (see, for example, ref. [22]). The observed neutral Higgs bosons are combined from the basic scalar fields as

$$\begin{aligned} \begin{pmatrix} h_1 \\ h_2 \\ h_3 \end{pmatrix} &= -\sqrt{2}R \begin{pmatrix} \text{Re}\phi_1^0 \\ \text{Re}\phi_2^0 \\ \text{Im}(s_\beta\phi_1^0 - c_\beta\phi_2^0) \end{pmatrix}, \\ R &= \begin{pmatrix} c_1 & -s_1c_2 & s_1s_2 \\ s_1c_3 & c_1c_2c_3 - s_2s_3 & -c_1s_2c_3 - c_2s_3 \\ s_1s_3 & c_1c_2s_3 + s_2c_3 & -c_1s_2s_3 + c_2c_3 \end{pmatrix} \end{aligned} \quad (14)$$

Here $c_i = \cos \alpha_i$, $s_i = \sin \alpha_i$. Our definition differs from that used in Ref. [22] by the sign minus in front of R in (14). The \mathcal{CP} conserving case is realized at $\alpha_2 = \alpha_3 = 0$, the last angle α_1 is related to the quantity α used for the case without \mathcal{CP} violation as $\alpha_1 \rightarrow \pi/2 - \alpha$, $h_1 \rightarrow h$, $h_2 \rightarrow A$, $h_3 \rightarrow -H$. Instead of α_1 , we use below the angle $\delta = \beta - (\pi/2 - \alpha_1)$.

We consider only the lightest Higgs boson h_1 having in mind the decoupling regime where $M_{H^\pm}, M_{h_2}, M_{h_3} \gg M_{h_1}$. Besides, we fix free parameter of 2HDM in the couplings of scalars with charged Higgs (see [21] for definition) just as it is in MSSM, $\lambda_5 = 2M_{H^\pm}^2/v^2 + g^2$. Last choice guarantees us negligibly small contribution of charged Higgs loops into the discussed couplings of lightest Higgs boson with light.

To describe couplings of the lightest Higgs boson h_1 with quarks and charged leptons we use the widespread “Model II” in which the ratios of these couplings to those in the minimal \mathcal{SM} (one Higgs doublet) are

$$\begin{aligned} \bar{u}h_1u &\rightarrow (\sin \delta + \cot \beta \cos \delta) \cos \alpha_2 - i\gamma^5 \cot \beta \cos(\delta - \beta) \sin \alpha_2, \\ \bar{d}h_1d, \bar{\ell}h_1\ell &\rightarrow (\sin \delta - \tan \beta \cos \delta) - i\gamma^5 \tan \beta \cos(\delta - \beta) \sin \alpha_2, \\ VVh_1 &\rightarrow \sin \delta - \sin \beta \cos(\delta - \beta)(1 - \cos \alpha_2). \end{aligned} \quad (15)$$

The effective couplings of Higgs boson with light G_i (3),(4) can be written via standard

loop integrals and the above mixing angles (see [1] for definitions).

$$\begin{aligned}
G^\gamma &= G_{SM}^\gamma \sin \delta + \frac{\alpha}{12\pi} \cos \delta \left[-\Phi_{1/2}(b) \tan \beta + 4\Phi_{1/2}(t) \cot \beta \right] + \text{scalars} \\
&- \frac{\alpha}{12\pi} (1 - \cos \alpha_2) \left[3\Phi_1^\gamma(W) \sin \beta \cos(\delta - \beta) + 4\Phi_{1/2}(t) (\sin \delta + \cot \beta \cos \delta) \right], \\
\tilde{G}^\gamma &= \frac{\alpha}{12\pi} \left[\Phi_{1/2}^A(b) \tan \beta + 4\Phi_{1/2}^A(t) \cot \beta \right] \cos(\delta - \beta) \sin \alpha_2, \\
G^Z &= G_{SM}^Z \sin \delta + \frac{\alpha}{4\pi} \left[v_b \Phi_{1/2}(b) \tan \beta + 2v_t \Phi_{1/2} \cot \beta \right] \cos \delta + \text{scalars} \quad (16) \\
&- \frac{\alpha}{4\pi} (1 - \cos \alpha_2) \left[\Phi_1^Z(W) \sin \beta \cos(\delta - \beta) + 2v_t \Phi_{1/2}(t) (\sin \gamma + \cot \beta \cos \delta) \right], \\
\tilde{G}^Z &= \frac{\alpha}{4\pi} \left[2v_t \Phi_{1/2}^A(t) \cot \beta - v_b \Phi_{1/2}^A(b) \tan \beta \right] \cos(\delta - \beta) \sin \alpha_2; \\
v_b &= -\frac{3 - 4s_w^2}{12s_w c_w}, \quad v_t = \frac{3 - 8s_w^2}{12s_w c_w}
\end{aligned}$$

The first lines in formulas for G_γ and G_Z give their form for the standard 2-doublet model without \mathcal{CP} -mixing. At large $\tan \beta$ the imaginary part of all these couplings (arising from the b -quark contribution) becomes essential. It gives phases ξ_i (2) which differ essentially from 0 or π . The corresponding values of effective scales Λ_i and phases ξ_i (5), (2) could be calculated easily from these equations. The word *scalars* means charged Higgs loop contribution, it is negligibly small in the discussed case, so we will not write it below.

Finally, all box diagrams include VVh vertex. Therefore the box contribution (10) to the amplitude changes as

$$B_\pm \rightarrow B_\pm^{SM} [\sin \delta - \sin \beta \cos(\delta - \beta) (1 - \cos \alpha_2)] . \quad (17)$$

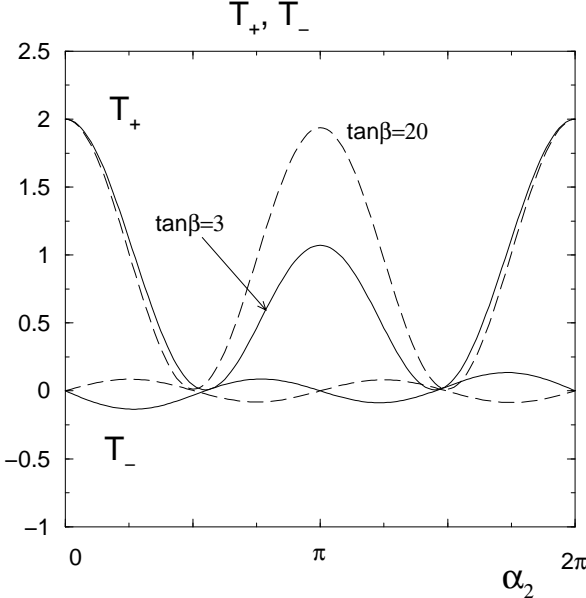


Figure 8: *Quantities T_\pm in 2HDM(II), $M_h = 110$ GeV. Strong \mathcal{CP} violation*

To make new effects more manifest, we study the dependence on two parameters α_2 and β only, keeping main features of discussed Higgs boson h_1 as close as possible to

the Higgs boson of \mathcal{SM} . For this purpose we fix parameter $\delta \approx \pi/2$ and consider small enough values of \mathcal{CP} -violated mixing angle α_2 . According to eq. (15), in this case couplings of h with quarks and gauge bosons are close to those in \mathcal{SM} (see refs. [23] for the detail discussion of this opportunity). In this case we have instead of previous equations

$$\begin{aligned} \bar{u}h_1u &\rightarrow \cos\alpha_2 - i\gamma^5 \cos\beta \sin\alpha_2, \quad \bar{d}h_1d \rightarrow 1 - i\gamma^5 \tan\beta \sin\beta \sin\alpha_2, \\ VVh_1 &\rightarrow 1 - \sin^2\beta(1 - \cos\alpha_2). \end{aligned} \quad (18)$$

$$\begin{aligned} G^\gamma &= G_{SM}^\gamma - \frac{\alpha}{12\pi}(1 - \cos\alpha_2) \left[3\Phi_1^\gamma(W) \sin^2\beta + 4\Phi_{1/2}(t) \right], \\ \tilde{G}^\gamma &= \frac{\alpha}{12\pi} \left[\Phi_{1/2}^A(b) \tan\beta + 4\Phi_{1/2}^A(t) \cot\beta \right] \sin\beta \sin\alpha_2, \\ G^Z &= G_{SM}^Z - \frac{\alpha}{4\pi}(1 - \cos\alpha_2) \left[\Phi_1^Z(W) \sin^2\beta + 2v_t\Phi_{1/2}(t) \right], \\ \tilde{G}^Z &= \frac{\alpha}{4\pi} \left[2v_t\Phi_{1/2}^A(t) \cot\beta - v_b\Phi_{1/2}^A(b) \tan\beta \right] \sin\beta \sin\alpha_2, \\ B_\pm &= B_\pm^{SM} [1 - \sin\beta \cos\beta(1 - \cos\alpha_2)]. \end{aligned} \quad (19)$$

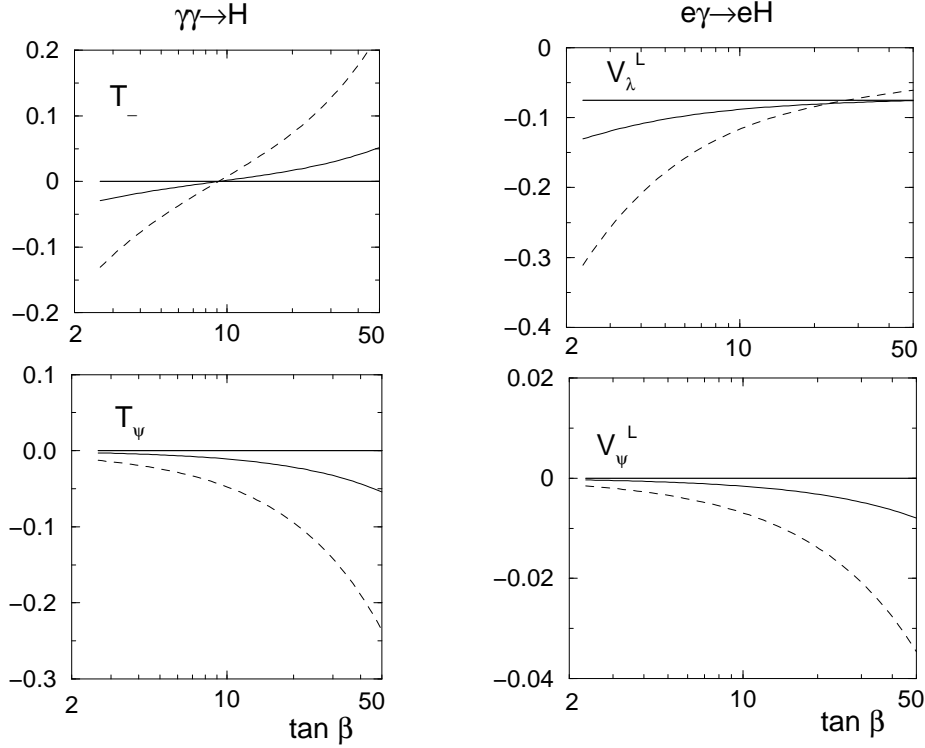


Figure 9: *Spin asymmetries in $\gamma\gamma \rightarrow h$ and $e\gamma \rightarrow eH$ processes due to scalar-pseudoscalar mixing in 2HDM(II), $M_h = 110$ GeV; for $e\gamma \rightarrow eH$ process $E_{tot} = 1.5$ TeV. The thick solid lines show the \mathcal{SM} values; thin solid and dashed lines refer to $\sin\alpha_2 = 0.1$ and 0.5 respectively*

Fig. 8 presents the overall dependence on α_2 . The strong oscillations might seem surprising. To explain them on the example of T_+ , let us first note that at $\alpha_2 \approx \pi/2$

and $\tan\beta \gg 1$ the boson h_1 becomes almost pseudoscalar. Next, it is well known that the two-photon decay width of the pseudoscalar is significantly smaller than the $h \rightarrow \gamma\gamma$ decay width. Therefore, quantity T_+ should be close to zero at $\alpha_2 \approx \pi/2$. For more details, one can consider this quantity T_+ for the case $\tan\beta = 3$, for definiteness. In this case $\sin^2\beta = 0.9$. By definition, $T_+ \propto |G|^2 + |\tilde{G}|^2$, the W contribution in the first term plays the dominant role everywhere except for narrow region near $\alpha_2 = \pi/2$ and thus dictates the shape $T_+ \propto [1 - 0.9(1 - \cos\alpha_2)]^2 + \text{small remnants}$. At α_2 slightly above $\pi/2$, when t -quark exactly cancels the remnant of W boson contribution (and the real part of the b contribution), T_+ is saturated by $|\tilde{G}|^2$, which is intrinsically smaller than $|G_{SM}|^2$ by two orders of magnitude. The shape of T_- , etc. dependence on α_2 can also be foreseen from Eq.(19) in the same way. Our calculations show that the quantities T_\perp , T_ψ as well as asymmetries V_i of the $e\gamma \rightarrow eH$ reaction also exhibit a similar oscillatory dependence on α_2 . The principal features of the results remain the same for other values of Higgs boson masses, including region $M_h > 2M_W$ above the WW threshold.

However, the case of strong \mathcal{CP} mixing is obviously so prominent that it will be seen at other colliders. The opposite case — the "weak mixing regime" (small values of α_2) — looks especially interesting. The above equations show that in this region T_- , T_ψ , $V_\psi \propto \alpha_2$, $V_\lambda \propto c\lambda_V + \alpha_2$, all other quantities differ from their values without \mathcal{CP} mixing only a little, by a quantity $\sim \alpha_2^2$. Therefore, the asymmetries T_- , T_ψ for $\gamma\gamma$ collisions and V_ψ , V_λ for γe collisions are most sensitive to the weak \mathcal{CP} mixing, as it is seen in Figures.

The quantities T_- and T_ψ are non-zero only due to \mathcal{CP} violation. Their $\tan\beta$ -dependence for different α_2 is shown in Fig. 9. The measurements of both of these quantities supplement each other essentially: asymmetry T_ψ is most sensitive to mixing effects at large $\tan\beta$, while in the small β domain the best suited quantity is T_- . This $\tan\beta$ dependence of the both quantities again can be traced from Eq.(19). Asymmetry T_- , being proportional to $\text{Re}(\tilde{G}_\gamma G_\gamma^*)$, borrows its $\tan\beta$ behavior from interplay of the b and t quark contributions to $\text{Re}(\tilde{G}_\gamma)$: the b contribution, initially small, grows with $\tan\beta$. It compensates the t loop at $\tan\beta \approx 10$ and becomes dominant later on. At the same time, T_ψ has $\tan\beta$ -dependence similar to $\text{Im}(\tilde{G}_\gamma)$, where we have only b quark loop contribution. Thus, the whole asymmetry T_ψ scales as $\tan\beta$.

For the γe collision we present only the quantities arising from \mathcal{CP} non-conservation, they are $\propto \alpha_2$ at small α_2 (Fig. 9). Just as for $\gamma\gamma$ reaction the studies of both these quantities supplement each other. The effect of circular polarization V_λ^L (which is an analogue to T_-) is relatively large at $\tan\beta \sim 1$, the t/b quark loop compensation point diminish this effect with growth of $\tan\beta$ (it becomes zero at large $\tan\beta$). Thus, in the whole $\tan\beta$ domain under investigation the t quark loop in \tilde{G}_i is dominant and therefore makes V_λ^L behave roughly as $\cot\beta$. Oppositely, the effect of linear photon polarization V_ψ^L (which is similar to T_ψ) is very small at $\tan\beta \sim 1$ but it grows with $\tan\beta$. Nevertheless, it stays below 0.05 and seems thus hardly measurable.

The obtained results describe also production of the lightest Higgs boson in the \mathcal{MSSM} in the decoupling regime (when all superparticles are heavy enough). It is necessary to note in this respect that the modern calculations in the \mathcal{MSSM} need to fix many subsidiary parameters. In the standard choice, the variation of Higgs mass and $\tan\beta$ shifts also quantity δ , so that curves of Ref. [7, 19], for example, present simultaneous dependence on parameters α_2 , β and δ . That is why numerical results of [7, 19] obtained for the specific problems discussed there differ from our Figs. 8,9. The numerical experiments show that simple variation of \mathcal{MSSM} parameters A and μ allows one to

have \mathcal{SM} like value $\sin \delta \approx 1$ at $M_h = 105 - 125$ GeV [24]. Our curves correspond to this very case of \mathcal{MSSM} .

6 Discussion

In this work, together with [1], we gave detailed answers to the questions what is the whole experimentaly available information about photon-Higgs boson anomalous interactions and how to extract it in a reasonable way from future experiments at Photon Colliders. Due to the absence of \mathcal{SM} couplings of the Higgs boson with photons at tree level, the signal of non-standard phenomena can appear very clean in Higgs boson production in photon collisions. The high sensitivity of reactions $\gamma\gamma \rightarrow H$ and $e\gamma \rightarrow eH$ to the admixture of various anomalous interactions makes these processes very useful in exploring the New Physics beyond TeV scale. With new degrees of freedom (2) in the parametric space, the unique opportunities of Photon Colliders in the variation of the initial photon polarization provide a new route to studying different anomalies in details and confident separation of different contributions.

The results presented shows the range of effects that could be resolved from the data, it is close to that for the \mathcal{CP} -even case [1]. They are $\Lambda_\gamma, \Lambda_{P\gamma} \sim 40 \div 60$ TeV for $H\gamma\gamma$ anomalies and $\Lambda_Z, \Lambda_{PZ} \sim 20$ TeV for $HZ\gamma$ anomalies⁴. Effects depend strongly on the phase of anomaly (2). The comparative study of effects with circularly and linearly polarized photons is necessary to separate effects of amplitude and phase of anomaly (Λ_i and ξ_i). Future simulations based on final versions of collider and detector will show the exact discovery limits before actual experiments.

Last, we analyzed some specific cases of anomalies: the presence of new particles within \mathcal{SM} (for \mathcal{CP} even anomalies, [1])⁵ and scalar-pseudoscalar mixing in the two-doublet Higgs model. Their important feature is definite relation among the anomalous signals in $\gamma\gamma$ and γe collisions. In particular, the study of both $\gamma\gamma$ and γe reactions is essential to test if we deal with either \mathcal{CP} violating mixing in 2HDM with definite relation among $H\gamma\gamma$ and $HZ\gamma$ anomalies or with some other mechanism of \mathcal{CP} violation with now unpredictable relation between these two anomalies. The specific feature of result is that signals of small mixing ($\sin \alpha_2 \sim 0.1$) are seen well in effects with circular photon polarization at small and large $\tan \beta$ (but not at intermediate, $\tan \beta \sim 10$), whereas effects with linear photon polarization can be seen well at intermediate and large values of $\tan \beta$.

We are thankful to V. Ilyin, M. Krawczyk, V. Serbo and P.Zerwas for discussions. IPI is thankful to Prof. J.Speth for hospitality at Forschungszentrum Jülich and IFG is thankful to Prof. A.Wagner for hospitality in DESY, where the paper was finished. This work was supported by grants RFBR 99-02-17211 and 96-02-96030, grant "Universities of Russia" 015.0201.16 and grant of Sankt-Petersburg Center of fundamental studies.

⁴ The relation of these scales to the scale of New Physics was discussed in Sec. 2

⁵ Note that "existence of extra chiral generations with all fermions heavier than M_Z is strongly disfavored by the precision electroweak data. However the data are fitted nicely even by a few extra generations, if one allows neutral leptons to have masses close to 50 GeV" [25]

References

- [1] A.T. Banin, I.F. Ginzburg, I.P. Ivanov, Phys. Rev. **D59** (1999) 115001 .
- [2] G.L. Kotkin, V.G. Serbo, Phys. Lett. **B413** (1997) 122.
- [3] B. Grzadkowski, F.J. Gunion, Phys. Lett. **B294** (1992) 361.
- [4] M. Kramer, J. Kuhn, M.L. Stong, P. Zerwas. Z. Phys. **C64** (1994) 21.
- [5] G.J. Gounaris, F.M. Renard, Z. Phys. **C69** (1996) 513.
- [6] E. Gabrielli, V.A. Ilyin, B. Mele, Proc. Phys. Rev. **D60** (1999) 113005; Proc. Int. Workshop on Linear Coll. Stiges, Spain(1999) hep-ph/9907574; hep-ph/9912321.
- [7] S.Y. Choi, J.S. Lee, hep-ph/9912330
- [8] E. Asakawa, J. Kamoshita, A. Sugamoto, I. Watanabe, hep-ph/9912373.
- [9] I.F. Ginzburg, G.L. Kotkin, V.G. Serbo, V.I. Telnov. Pis'ma ZhETF **34** (1981) 514. Nucl. Instr. Methods (NIM) **205** (1983) 47. I.F. Ginzburg, G.L. Kotkin, S.L. Panfil, V.G. Serbo, V.I. Telnov. NIM **219** (1984) 5.
- [10] Zeroth-order Design Report for the NLC, SLAC Report 474 (1996); R. Brinkmann et. al., NIMR **A406** (1998) 13.
- [11] I.F. Ginzburg, G.L. Kotkin, Eur. Phys. J. **C13** (2000) 295; hep-ph/9905462.
- [12] M. Melles, W.J. Stirling, V.A. Khoze, Phys. Rev **D61** (2000) 054015; G. Jikia, S. Söldner-Rembold, Proc. PHOTON'99, in print; hep-ph/9910366.
- [13] B. Grzadkowski, F.J. Gunion, J. Kalinowski, Phys. Rev. **D60** (1999) 075011.
- [14] W. Buchmuller, D. Wyler. Nucl. Phys. **B264** (1986) 621; C.I.C. Burges, H.I. Schnitzer. Nucl. Phys. **B228** (1983) 464; C.N. Leung, S.T. Love, S. Rao. Z. Phys. **C31** (1986) 433.
- [15] K. Hagiwara et al, Phys. Rev. **D 48** (1993) 2182.
- [16] M. Spira, Fortsch. Phys. **46** (1998) 203.
- [17] E. Gabrielli, V.A. Ilyin, B. Mele, Phys. Rev. **D56** (1997) 5945.
- [18] M. Savci, J. Phys. **G23** (1997) 797.
- [19] U. Cotti, J.K. Diaz-Cruz, J.J. Toscano, hep-ph/9912406.
- [20] V.M. Budnev, I.F. Ginzburg, G.V. Meledin, V.G. Serbo, Phys. Rep. **15C** (1975) 181; I.F. Ginzburg, V.G. Serbo, Phys. Lett. **103B** (1981) 68.
- [21] J.F. Gunion, H.E. Haber, G.L. Kane, S. Dawson. *The Higgs Hunter's Guide*, Addison-Wesley, Reading (1990).
- [22] B. Grzadkowski, J.F. Gunion, J. Kalinowski. Phys. Rev. **D60** (1999) 075011.

- [23] I.F. Ginzburg. Proc. Conf. PHOTON'99, Freiburg (1999), hep-ph/9907549;
I.F. Ginzburg, M. Krawczyk, P. Olsen, hep-ph/9909455
- [24] I.F. Ginzburg, M. Krawczyk, P. Olsen, in progress.
- [25] M.Maltoni, V.A. Novikov, L.B. Okun, A.N. Rozanov, M.I. Vysotsky, hep-ph/9911535.